Lifetime and Coherence of Two-Level Defects in a Josephson Junction

Yoni Shalibo,[1] Ya'ara Rofe,[1] David Shwa,[1] Felix Zeides,[1] Matthew Neeley,[2] John M. Martinis,[2] and Nadav Katz[1]

[1]*Racah Institute of Physics, The Hebrew University of Jerusalem, Jerusalem 91904, Israel*

[2]*Department of Physics, University of California, Santa Barbara, California 93106, USA*

(Received 14 July 2010; published 19 October 2010)

We measure the lifetime (T_1) and coherence (T_2) of two-level defect states (TLSs) in the insulating barrier of a Josephson phase qubit and compare to the interaction strength between the two systems. We find for the average decay times a power-law dependence on the corresponding interaction strengths, whereas for the average coherence times we find an optimum at intermediate coupling strengths. We explain both the lifetime and the coherence results using the standard TLS model, including dipole radiation by phonons and anticorrelated dependence of the energy parameters on environmental fluctuations.

DOI: 10.1103/PhysRevLett.105.177001 PACS numbers: 74.50.+r, 03.65.Yz, 77.84.Bw, 85.25.Dq

Two-level defects in amorphous insulators are of fundamental interest due to their impact on many low temperature properties, such as heat conductivity [1] and the generation of $1/f$ noise [2,3]. On the practical side, these effects limit the operation of solid state devices, for example, amplifiers [4] and CCD detectors [5], and increase the dielectric loss of insulators [6].

Recently, a new type of solid state device has emerged in which quantum coherence is maintained over a large distance. In particular, superconducting Josephson qubits allow one to study quantum coherence at the macroscopic level [7]. Two-level defects in their amorphous oxide tunnel barriers [usually made of AlO_x ($x \approx 1$) [8]] have been found to limit the performance of these devices [6,9,10]. In the phase qubit, it was found that at certain biases the qubit is strongly coupled to spurious two-level states (TLSs) which result in free oscillations with the qubit and effectively reduce its coherence [11]. Similar effects have been observed in the flux qubit as well [12], although these are less common due to its smaller junction. Superconducting qubits hold promising features for the implementation of quantum information processing devices; however, a significant improvement in the defect density is required for future progress.

These defects are thought to arise from charge fluctuators in the insulating material of the junction, presumably O-H bonds [6]. Measurements on dielectrics at high temperature and power combined with measurements on the phase qubit at low temperature strongly support a two-level model for these fluctuators, emerging from tunneling between two configurational states of the charge inside the junction. The notion of coupling of the phase qubit to a strongly anharmonic microscopic system was further fortified through careful analysis of the multilevel spectrum of the phase qubit near resonance with a defect [13]. Neeley *et al.* have demonstrated coherent control over a single defect, and characterized its coherence and relaxation time [14]. Other attempts are being made to reduce the impact of defects by improving junction materials using epitaxial growth [15] or by fabricating dielectric free junctions [16].

Several mechanisms have been proposed for relaxation and dephasing of the dielectric defects themselves. Energy relaxation is caused by coupling to phonon states, while dephasing could be caused by spectral diffusion [1]. However, to date, only limited measurements were carried out on TLSs to characterize these processes at the single defect level [17]. Such measurements could be used to better understand the nature of the defects and their decay mechanisms, and possibly engineer long-lived quantum memories in future devices. In [17], the coherence times of several TLSs were measured spectroscopically and were found to distribute as $P \sim 1/T_2$, where T_2 is the spectroscopic coherence time. Neeley's method [14] of probing the TLS adds the capability of measuring the coherence time more accurately and also measuring their lifetime separately.

In this Letter, we present a measurement of the decay of energy and coherence for a large ensemble of TLSs in a small area junction using the phase qubit. We find that on average, the energy relaxation time (T_1) follows a power-law dependence on the coupling parameter to the phase qubit. The exponent of this power law is in fair agreement with what is expected from phonon radiation by a dipole (proportional to the coupling strength) inside the junction. The average dephasing time [$T_\phi = (1/T_2 - 1/2T_1)^{-1}$] is coupling dependent as well, peaking at intermediate couplings. We interpret this optimum coupling to be caused by anticorrelated fluctuations in the physical parameters which determine the TLS energy.

For small area junctions ($\sim 1\ \mu m^2$), the typical measurement bandwidth allows us to detect and measure about 10 TLSs in a particular cooldown. Instead of using many different samples to acquire sufficient statistics, we use the fact that heating resets the TLS characteristics. The device is thermally anchored to the mixing chamber of a dilution refrigerator during measurement. We find that the TLS

distribution is reset upon raising the temperature above 20 K and cooling down to the base temperature (10 mK). Some memory of the TLS distribution remains if the temperature is increased to only 1.5 K [18]. We utilize this feature to produce a new set of TLSs and generate an ensemble. The data were taken over 82 different TLSs, obtained from 8 different cooldowns.

The initial identification of TLSs and their coupling parameters are carried out as follows. First, the qubit spectrum is swept over the bias [19] to locate the frequencies of TLSs from the positions of the avoided level crossing structures [see Fig. 1(a)]. A complementary picture of the interacting qubit-TLS system in the time domain is shown in Fig. 1(b), where we excite the qubit with a short resonant pulse (π pulse) far away from any observable TLS and then apply a bias pulse of varying amplitude and length. As seen in the figure, for bias values where the qubit is resonant with a TLS we observe oscillations that have the same frequency as the splitting size in the spectrum.

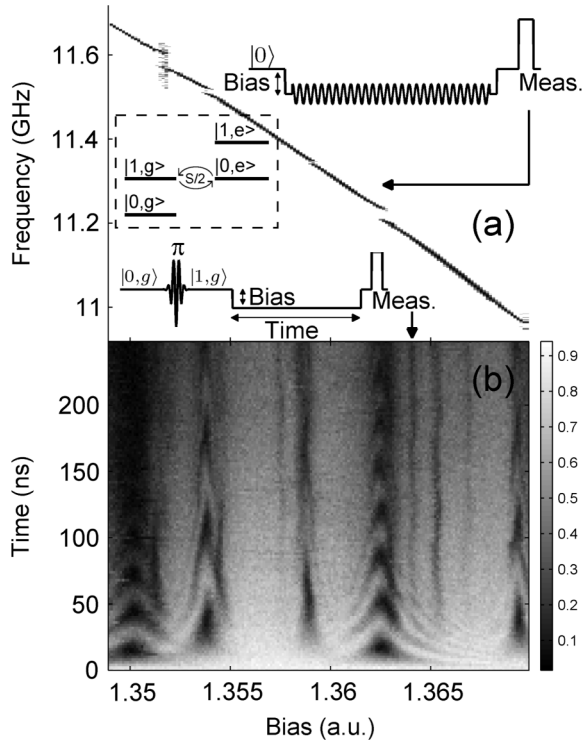

FIG. 1. Frequency-domain and time-domain signatures of TLSs in qubit measurement. (a) The probability of the qubit being excited (P_1, normalized) after a long microwave tone at different frequencies and biases. On top of the expected smooth change of qubit frequency with bias, we observe randomly scattered splittings due to coupling to TLSs. (b) P_1 after qubit excitation followed by a "free" evolution at different bias values. P_1 oscillates near resonance with TLSs, consistent with the position of splittings in the spectrum. Upper and lower insets: control sequences used to produce (a) and (b), respectively. $|0, g\rangle$ and $|1, g\rangle$ stand for states where the qubit is at its ground and excited state, respectively, while the TLS is at its ground state. Dashed inset: level diagram for the combined qubit-TLS system on resonance.

Following Neeley *et al.* [14], the characteristic energy relaxation and decoherence time scales were extracted from T_1 and Ramsey experiments on the TLS, with sequences schematically represented in the insets of Fig. 2. Figures 2(a) and 2(b) show representative T_1 and T_2 decay curves of the same TLS with characteristic times of 187 and 148 ns, respectively, obtained from a fit to a decaying exponent and an oscillatory decaying exponent. The size distribution of the observed splittings [see Fig. 3(a)] follows the theoretical curve predicted by the standard model for two-level defects and agrees with previous results on similar junctions (generated by measuring different samples) [6]. The maximal splitting size is found to be 45 MHz. Theory predicts [6] that this maximal splitting $S_{\max}$ depends on junction parameters and defect size according to $S_{\max} = (2d/x)\sqrt{e^2 E_{10}/2C}$, where x is the barrier thickness, d is the spatial size of the dipole, C is the junction capacitance, and E_{10} is the qubit energy. From the measured $S_{\max}$ and known junction parameters we compute a dipole size $d \simeq 1$ Å. The minimal observable splitting size is $\sim$3 MHz, and is mainly limited by the coherence time of the qubit. In addition, we find the distribution of TLS energies (E_{ge}, the energy between the ground state and excited state) to be constant throughout our qubit measurement bandwidth [see Fig. 3(b)], consistent with theory.

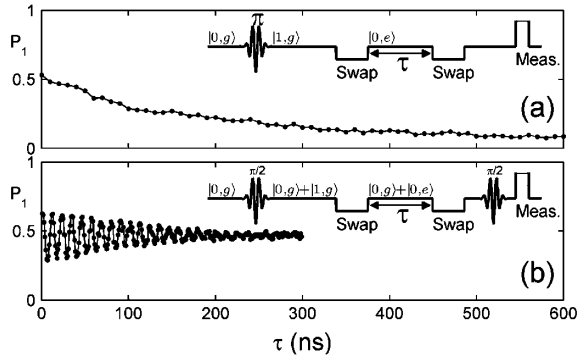

FIG. 2. Representative T_1 and T_2 measurements of a TLS. (a) T_1 measurement of the TLS, along with its experimental sequence (inset). The qubit is first excited with a π pulse, then brought into resonance with a TLS for a "swap time" [the time to fully transfer an excitation between the qubit and the TLS; it is found for each TLS by locating the first minimum in the oscillations in Fig. 1(b)]. After a free evolution of the TLS of time τ, a swap gate is again applied, after which the qubit excitation probability P_1 is measured. (b) T_2 measurement of a TLS, along with its experimental sequence (inset). This sequence is similar to a T_1 measurement, only that superposition states are produced in the TLS and their decay is measured vs time (Ramsey sequence [14]). The amplitude of the oscillations is proportional to the degree of coherence in the TLS.

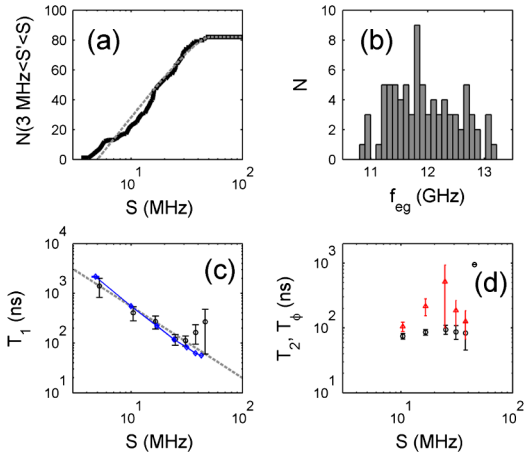

FIG. 3 (color online). TLS survey results. (a) Frequency and (b) splitting-size distribution of 82 TLSs. The curve in (a) is the best-fitted log-normal distribution of the standard TLS model [6]. (c) Average T_1 values (black circles) as a function of average splittings taken for TLSs inside a 7 MHz splitting window, and the best-fitted power law in dashed gray. Average T_1 from stochastic simulation (arbitrary amplitude is shown) in blue diamonds. We attribute the deviation at the largest splittings to low statistics within these windows [18] (d) Average T_2 (black circles) and T_ϕ (red triangles) value as a function of average splitting-size within a 7 MHz window.

Although most of the T_1 decay curves of the TLSs are similar in their shape (i.e., a simple exponential decay), their decay times range almost 3 orders of magnitude, from 12 ns to more than 6000 ns. Coherence times on the other hand range from 30 ns to only 150 ns (excluding a single anomalous TLS which will be discussed later). For comparison, when the qubit is biased far from any observable splitting, its lifetime is 270 ns, and its coherence time is 90 ns. TLS energy relaxation times at a given splitting are not random. We find that they are shorter for larger splittings (stronger interaction with the qubit), although short lifetimes are measured for the smallest splittings as well. This trend is apparent in Fig. 3(c) where we plot average T_1 values as a function of splitting. In this plot we divide the ensemble into groups of TLSs having similar splitting values, in a 7 MHz window size. The error bar represents the statistical spread of the data within this window [18]. We find the average values $\langle T_1(S)\rangle$, excluding two points [18], to be best fitted by a power law $T_1 \propto S^\alpha$, where $\alpha = -1.44 \pm 0.15$ [18]. Figure 3(d) (black circles) shows the processed T_2 data, obtained similarly from only 43 different TLSs [18]. In this case we observe a weak dependence on the coupling with a peak at $S \approx 25$ MHz. This feature is more pronounced in the dephasing time T_ϕ, represented by red triangles in Fig. 3(d).

The T_1 results can be understood within the standard TLS model. The excited state of the TLS involves a local deformation of the insulator. This deformation couples to phonon modes, leading to the decay of the TLS excitation. The expected lifetime for such a process [1], is given by

$$T_1^{-1} = \frac{E_{\rm ge}\Delta_0^2\gamma^2}{2\pi\rho\hbar^4}\left(\frac{1}{v_l^5} + \frac{2}{v_t^5}\right), \quad (1)$$

where γ is the deformation potential, v_l and v_t are the speeds of sound for the longitudinal and transverse modes, respectively, Δ_0 is the energy splitting due to tunneling, and ρ is the mass density. This is consistent with a power-law dependence on S, since the interaction strength with the qubit satisfies $S \propto S_{\rm max}\Delta_0/E_{\rm ge}$ [6].

The interaction of a TLS with the qubit is that of an electric dipole with an electric field, and therefore depends on the dipole orientation [6]. This feature explains the large spread in the data at a given splitting: both large dipoles (large $\Delta_0/E_{\rm ge}$) perpendicular to the junction's electric field and small dipoles aligned with the field can have the same S but different lifetimes. To more rigorously compare experiment with this theory, we simulate an ensemble of TLSs with uniform distribution of dipole orientation and log distribution of dipole moment sizes [6], from which we calculate the average lifetimes as a function of splitting size [18]. The simulation data [see Fig. 3(c)] yield an average exponent $\alpha = -1.63$ [18], in agreement with our measurement.

The magnitude of the times that we extract from the experiment at a given splitting can be compared to the expected values for defects inside an AlO_x dielectric using Eq. (1). We approximate the deformation potential by $\gamma = \frac{1}{2}\rho v^2 \Delta V$ [21], where v is the average speed of sound of the transverse and longitudinal modes and ΔV is the local difference in volumes. For Al_2O_3 values with the difference in volumes taken as $\Delta V \simeq a^3$, where $a \simeq 1$ Å is the extracted dipole size, we get $\gamma \approx 1$ eV, consistent with defects in other dielectrics [3]. Since the dielectric layer thickness is much smaller than the relevant phonon wavelength, the speed of sound in Eq. (1) is set by the aluminum layers of the electrodes. Using the speed of sound for thin aluminum films [22], we get $T_1(S_{\rm max}) \simeq 30$ ns which is very similar to what we measure. A more specific estimation should take into account the size of the junction and the layered structure.

Assuming the dephasing process is caused by fluctuations in energy, we note that the maximum observed in Fig. 3(d) can be explained by an anticorrelated dependence of the charging energy and tunneling energy on fluctuations in the TLS environment. According to the TLS model, $E_{\rm ge} = \sqrt{\Delta^2 + \Delta_0^2}$ where Δ is the energy difference between the bare states of two spatial configurations $|L\rangle$ and $|R\rangle$, and Δ_0 is the tunneling interaction energy. Both Δ and Δ_0 are dependent on a set of environmental parameters $\vec{P}$, which fluctuate in time. As is standard for the TLS model, we assume a linear sensitivity for Δ on $\vec{P}$ and an exponential sensitivity for Δ_0 : $\Delta_0(\vec{P}) = N_1 e^{-\sum P_i/P_{0i}}$, $\Delta(\vec{P}) = N_2 \sum P_i/P_{1i}$, with overall dimensional normalization constants N_1 and N_2 and parameter specific constants

$\vec{P}_0$ and $\vec{P}_1$. The resulting fluctuations in energy, to first order in fluctuations $\delta\vec{P}$ in these parameters, are given by $\delta E_{\rm ge} = \frac{1}{E_{\rm ge}} \sum \delta P_i (\Delta^2/P_{1i} - \Delta_0^2/P_{0i})$. This expansion becomes interesting for the situation where $\Delta_0 \sim \Delta$ as there is a possibility for the contribution in $\delta E_{\rm ge}$ to pairwise cancel. Since $\Delta_0 = (E_{\rm ge}/S_{\rm max}\cos\eta)S$, where η is the dipole orientation relative to the junction's electric field, we expect to find such a cancellation at a particular splitting S. Note that the dependence on $\cos\eta$ smears this somewhat, but we still expect a significant effect, as is observed in Fig. 3(d).

As seen in the figures, the power law describing $T_1(S)$ cannot explain all the measured TLSs. We find that three out of 82 TLSs with large splittings (37 MHz, 41 MHz, and 45 MHz) have much longer lifetimes than expected (220, 243, and 476 ns, respectively). In addition, one TLS out of 41 has much longer coherence than all the others (about a factor of 6 longer than the longest T_2 of all the others), associated with a splitting of size 30 MHz. Other anomalies we discovered are related to the stability of a particular TLS in time. We find that the energy $E_{\rm ge}$ of some TLSs (about 5%) changes spontaneously at varying time scales, from seconds to days. All the rest were remarkably stable [18].

Some of these changing TLSs have long lifetime (a few microseconds), which is consistent with the power-law trend we discussed above. Furthermore, we also measure a few representative TLSs as a function of temperature. We find no significant change in T_1 and T_2 below 100 mK, consistent with the expected [1] $\tanh(E_{\rm ge}/2k_BT)$ dependence. We also find that the instability of some TLSs increases at elevated temperatures (i.e., the change in TLS energy becomes more frequent). We conclude that some of the TLSs we measure have a different nature, perhaps related to their internal structure or position inside the junction.

In conclusion, the energy decay and dephasing times of two-level defects in an AlO_x barrier of a Josephson junction are measured as a function of the coupling parameter with the phase qubit. The lifetimes vary substantially in our range of splittings, and agree with the theoretically predicted phonon radiative loss, which is dipole size dependent. The dephasing times show an extremum at intermediate couplings, which we attribute to an anticorrelated dependence on fluctuations in the environmental parameters which set the TLS energy. Such a dependence may distinguish between different theoretical models for TLSs. Our results demonstrate the power of the phase qubit as a dynamical coupling element to microscopic systems at the single microwave photon level.

We acknowledge fruitful discussions with Clare C. Yu. This work was supported by ISF Grant No. 1835/07 and BSF Grant No. 2008438.

[1] W. A. Phillips, Rep. Prog. Phys. **50**, 1657 (1987).
[2] A. Shnirman, G. Schon, I. Martin, and Y. Makhlin, Phys. Rev. Lett. **94**, 127002 (2005).
[3] L. C. Ku and C. C. Yu, Phys. Rev. B **72**, 024526 (2005).
[4] M. J. Kirton *et al.*, Semicond. Sci. Technol. **4**, 1116 (1989).
[5] N. Saks, IEEE Electron Device Lett. **1**, 131 (1980).
[6] J. M. Martinis *et al.*, Phys. Rev. Lett. **95**, 210503 (2005).
[7] J. Clarke and F. K. Wilhelm, Nature (London) **453**, 1031 (2008).
[8] E. Tan, P. G. Mather, A. C. Perrella, J. C. Read, and R. A. Buhrman, Phys. Rev. B **71**, 161401 (2005).
[9] K. B. Cooper *et al.*, Phys. Rev. Lett. **93**, 180401 (2004).
[10] E. Lucero *et al.*, Phys. Rev. Lett. **100**, 247001 (2008).
[11] R. W. Simmonds *et al.*, Phys. Rev. Lett. **93**, 077003 (2004).
[12] A. Lupascu, P. Bertet, E. F. C. Driessen, C. J. P. M. Harmans, and J. E. Mooij, Phys. Rev. B **80**, 172506 (2009).
[13] P. Bushev *et al.*, arXiv:1005.0773.
[14] M. Neeley *et al.*, Nature Phys. **4**, 523 (2008).
[15] S. Oh *et al.*, Phys. Rev. B **74**, 100502 (2006).
[16] G. Tettamanzi *et al.*, in *Proceedings of the 2006 International Conference on NanoScience and Nanotechnology* (IEEE, New York, 2006).
[17] T. A. Palomaki *et al.*, Phys. Rev. B **81**, 144503 (2010).
[18] See supplementary material at http://link.aps.org/supplemental/10.1103/PhysRevLett.105.177001 for a complete data set and discussion about data fitting, temperature dependence, and stochastic simulation.
[19] The qubit loop is coupled to an external bias source through a flux transformer, which sets the qubit energy [20].
[20] J. M. Martinis, S. Nam, J. Aumentado, and C. Urbina, Phys. Rev. Lett. **89**, 117901 (2002).
[21] J. P. Sethna, Phys. Rev. B **25**, 5050 (1982).
[22] W. M. Haynes, *CRC Handbook of Chemistry and Physics* (CRC Press, London, 2010), 91st ed., ISBN 1439820775.